AN ABSTRACT OF THE THESIS OF

Dominic Jude Ogbonnah for the degree of Master of Science

in Chemical Engineering presented on December 16, 1976

Title: AMMONIA ABSORPTION FROM ENTRAINED BUBBLES PRODUCED

BY LIQUID PLUNGING JET

Redacted for Privacy

Abstract approved: _____

Charles E. Wicks

A mathematical model was used to study gas absorption from entrained ammonia bubbles produced by liquid plunging jets in water. The transfer factor, TF, defined as the product of the interfacial area and the overall liquid mass transfer coefficient, summed over all the entrained bubbles was experimentally determined using this model. The experimental investigation ranged from jet stream Reynolds number of 10,887 to 19,643, and Weber number of 233 to 944. Three different jet nozzles of diameters 0.225 cm, 0.540 cm and 0.680 cm were used in the experimental investigation. The transfer factor, TF, was successfully correlated with the product of the Reynolds number, N_{Re}, and Weber number, N_{We}. The product of these two dimensionless numbers, $N_{Re} \times N_{We}$, is equivalent to the rate at which the jet stream supplies kinetic energy to the pool. Specifically, TF

was correlated to be:

$$TF = 8.3532 \exp(0.1278 \times 10^{-6} N_{Re} N_{We}).$$

The above correlation for TF was obtained for the absorption of ammonia in water. The experimental investigation was carried out at a total gas pressure of 770 mm Hg and pool temperature of 21.1°C. Comparison of the results obtained in the present project with data reported in the literature confirmed the fact that TF is an inverse function of the solubility.

Ammonia Absorption from Entrained Bubbles Produced by Liquid Plunging Jet

by

Dominic Jude Ogbonnah

A THESIS

submitted to

Oregon State University

in partial fulfillment of

the requirements for the

degree of

Master of Science

Completed December 16, 1976

Commencement June 1977

APPROVED:

Redacted for Privacy

Professor of Chemical Engineering
in charge of major

Redacted for Privacy

Head of Department of Chemical Engineering

Redacted for Privacy

Dean of Graduate School

Date thesis is presented December 16, 1976

Typed by Kathy McKee for Dominic Jude Ogdonnah

ACKNOWLEDGMENT

The author would like to thank:

Dr. C. E. Wicks for his guidance throughout this project.

Mr. William B. Johnson for his assistance with equipment construction.

His parents for their letters of support and encouragement.

TABLE OF CONTENTS

LIST OF ILLUSTRATIONS

AMMONIA ABSORPTION FROM ENTRAINED BUBBLES PRODUCED BY LIQUID PLUNGING JET

INTRODUCTION

In many industrial processes involving gases and liquids, the gas has to be absorbed by the liquid as one of the steps in the overall operation. For example, wastewater treatment and alcohol production by fermentation require oxygen in substantial amounts. The rate of oxygen transfer is sometimes the rate controlling step in fermentation processes. There are also some industrial reactions where the rate of gas absorption is the controlling step. One way to increase the rate of gas absorption in the liquid is to create gas-liquid dispersions. The increased rate of absorption is due to the large surface area of the bubbles produced per unit volume of liquid in such dispersions. Various contacting devices are now in use which take advantage of the large surface areas of the bubbles in gas-liquid dispersions to enhance gas absorption.

Jackson (7) studied the mass transfer characteristics of Bernoulli-type devices in which gas-liquid dispersions were created and noted significantly high rates of mass transfer.

Calderbank (1) studied the rate of mass transfer from bubbles produced with the aid of impellers as used in most fermenters. He also studied mass transfer from bubbles using perforated plate gas dispensers, as in sieve plate trays. He concluded that the mass transfer coefficient in the liquid phase was not affected by mechanical agitation of the liquid when absorbing sparingly soluble gas. Accordingly, the results obtained were equally applicable in gas-liquid dispersions produced either with the aid of impellers

or perforated plates. The differences in performance with a given fluid system was attributed to the different interfacial areas produced by the two devices.

Lin and Donnelly (9) studied the entrainment of bubbles produced by liquid plunging from a vertical jet into a quiescent surface of the same liquid. Twelve Newtonian liquids, with viscosities ranging from 0.9 to 400 centipoise, surface tension varying from 30 to 63 dynes/cm and densities ranging from 0.876 to 1.246 g/cc, were used. The entrained gas was mostly air but carbon dioxide was also used in order to study the effect of gas properties on the entrainment process. The temperature of the fluid was maintained at 25 ± 1°C. The observed bubble sizes varied from 0.5 to 3 mm. The frequency of bubbble formation was from 0.5 to over 2,000 bubbles/sec. For some of the runs, especially with the low viscosity liquids, the rate of bubble formation was so high that it was not feasible to determine the formation frequency. Gas entrainment was observed to occur only when the average jet velocity exceeded a certain critical value that was called the minimum entrainment velocity. Although both laminar and turbulent jet streams were studied, the bulk of the studies was centered on entrainment produced from laminar plunging jets. From their experimental results, the following equation was developed to predict the minimum entrainment velocity for laminar plunging jets:

$$\text{Weber Number} = 10(\text{Reynolds Number})^{0.74}$$

Different jet nozzle sizes were used in this study. However, no

mass transfer studies were conducted in their experiments.

Swiggett (14) and Hauxwell (5) studied the mass transfer characteristics of the entrained bubbles produced by liquid plunging jets for slightly soluble gases. They noted high rates of mass transfer from the bubbles and successfully correlated their data using the Weber number and the Reynolds number. The absorption of oxygen, nitrogen and carbon dioxide in water was investigated.

The objective of this paper is to study the mass transfer characteristics of bubbles produced by liquid plunging jets when the gas used is soluble in the liquid.

THEORETICAL ANALYSIS

Consider a tank partially filled with water, into which a jet of water is plunging. The space above the water is filled with ammonia. If the water in the tank is taken as the control volume, then the following conservation law holds:

$$\left\{\begin{array}{l}\text{Rate of}\\ \text{accumula-}\\ \text{tion of}\\ \text{ammonia}\\ \text{in the}\\ \text{control}\\ \text{volume}\end{array}\right\} = \left\{\begin{array}{l}\text{Rate of}\\ \text{input of}\\ \text{ammonia}\\ \text{into the}\\ \text{control}\\ \text{volume}\end{array}\right\} - \left\{\begin{array}{l}\text{Rate of}\\ \text{discharge}\\ \text{of ammonia}\\ \text{from the}\\ \text{control}\\ \text{volume}\end{array}\right\} \qquad (1)$$

Ammonia can be transferred into the control volume by four different mechanisms:

a) Ammonia can be transferred into the control volume from the surface of the entrained bubbles produced as the liquid plunges into the volume control. This will be called R_b.

b) Ammonia can be transferred across the 'free' surface of the liquid into the control volume. The 'free' surface here is the interface between the gas and the liquid in the tank. This will be called R_s.

c) Ammonia also can be transferred into the control volume by being absorbed into the exposed surface

of the plunging liquid, just before it enters the control volume. This will be called R_j.

d) Ammonia also can be introduced into the control volume by the plunging liquid itself, flowing at a rate of Q_n liters/min and having a concentration of Cn $\frac{\text{g moles}}{\text{liters}}$. This will be called R_n. Hence $R_n = Q_n C_n \frac{\text{g moles}}{\text{min}}$.

Hence, the rate of input of ammonia into the control volume is equal to

$$R_b + R_s + R_j + Q_n C_n.$$

As ammonia is absorbed into the control volume, the concentration of ammonia within the pool changes. If C_o is the concentration of the liquid in $\frac{\text{g moles}}{\text{liter}}$, leaving the control volume at a flow rate of $Q_o \frac{\text{liters}}{\text{min}}$, the rate of discharge of ammonia from the control volume is $Q_o C_o$. If the volume of liquid in the control volume is V liters and its concentration is $C_1 \frac{\text{g moles}}{\text{liter}}$, the rate of accumulation of ammonia within the control volume is $\frac{d}{dt}(VC_1)$. Substituting these terms into equation (1), we have:

$$\frac{d}{dt}(VC_1) = R_b + R_s + R_j + Q_n C_n - Q_o C_o \qquad (2)$$

If the volume of the liquid is maintained constant, equation (2) becomes:

$$V\frac{dC_1}{dt} = R_b + R_s + R_j + Q_n C_n - Q_o C_o \qquad (3)$$

The Whitman 'two-film' theory can be used to model the rate of absorption from the bubbles, R_b. Basically this theory states that the diffusional resistance to gas-liquid mass transfer lies in the

individual fluid phases with no resistance at the gas-liquid interface. This implies that there should be no accumulation or depletion of the diffusing species at the boundary. This further implies that equilibrium concentration values should prevail at the gas-liquid interface. To study the rate of absorption from the bubbles, a single representative bubble will be modeled. Consider some j^{th} bubble (mostly pure ammonia gas, containing a slight amount of water vapor). This bubble has an area A_j which is in direct contact with the liquid in the control volume. Gas is absorbed from this bubble through a liquid film, with boundary concentration C_{ij} at the gas-liquid interface and C_{Lj} where the film contacts the bulk liquid. Hence for the j^{th} bubble, we have:

$$R_b = k_{Lj}A_j(C_{ij} - C_{Lj})$$

where k_{Lj} is the liquid film mass transfer coefficient for the j^{th} bubble. C_{ij} may or may not be equal to the equilibrium value C*, depending on the resistance to mass transfer in the gas phase. If the contents of the control volume are perfectly mixed, $C_Lj = C_L$. To avoid the question of gas phase resistance, the overall mass transfer concept of the two film model will be used. Considering all of the n entrained bubbles, we obtain

$$R_b = \sum_{j=1}^{n} k_{Lj}A_j(C_{ij} - C_L) = \sum_{j=1}^{n} K_{Lj}A_j(C^* - C_L).$$

To evaluate R_b, we will need to know the product of the mass transfer coefficient and the area of each bubble. This is difficult due to the swarms of bubbles; accordingly, a practical

representation involves lumping the sum of the product of the mass transfer coefficient and the area for all the bubbles as a transfer factor, TF,

$$TF = \sum_{j=1}^{n} K_{Lj} A_j$$

$$R_b = TF(C^* - C_L) \ .$$

The idea of transfer factor has been used successfully by Jackson (7) and Hauxwell (5).

For the rate of gas absorption across the 'free' surface, we have:

$$R_s = K_s A_s (C^* - C_L)$$

where

A_s = area of the gas-liquid interface

K_s = overall mass transfer coefficient

C^* = equilibrium concentration of ammonia at the liquid interface

C_L = concentration of ammonia in the control volume.

If the area of the plunging liquid exposed to the gas is very small and the contact time is short, R_j will be negligible. Substituting for R_b and R_s into equation (3), we have:

$$V\frac{dC_L}{dt} = TF(C^* - C_L) + K_s A_s (C^* - C_L) + Q_n C_n - Q_o C_o \ .$$

From the assumption of perfect mixing $C_L = C_o = C$ which permits further simplification of the model to:

$$V\frac{dC}{dt} = TF(C^* - C) + K_sA_s(C^* - C) + Q_nC_n - Q_oC \quad . \tag{4}$$

Since the volume of liquid in the control volume is constant, $Q_n = Q_o$. K_sA_s can be represented as a surface transfer factor, TFS. Equation (4) reduces to:

$$V\frac{dC}{dt} = TF(C^* - C) + TFS(C^* - C) + QC_n - QC \quad . \tag{5}$$

If the ammonia discharge stream, C_o, is recycled and used as the input stream to the control volume; $C_n = C_o = C$. Hauxwell (5) tested this assumption and found it to be true in his experimental investigations. Equation (5) now reduces to:

$$V\frac{dC}{dt} = TF(C^* - C) + TFS(C^* - C) \tag{6}$$

Dividing equation (6) by VC^*, we obtain

$$\frac{dC^+}{dt} = \frac{TF}{V}(1 - C^+) + \frac{TFS}{V}(1 - C^+) \tag{7}$$

where

$$C^+ = \frac{C}{C^*} \quad .$$

Simplifying equation (7), we obtain:

$$\frac{dC^+}{dt} = \frac{(TF + TFS)}{V}(1 - C^+) \tag{8}$$

$$\frac{dC^+}{(1 - C^+)} = \frac{(TF + TFS)}{V}\,dt$$

If TF and TFS are assumed to be terms independent of the concentration, equation (8) can be integrated subject to the following boundary conditions:

$$t = 0,\ C^+ = C_o^+$$

$$t = t,\ C^+ = C^+$$

$$\ell n \left[\frac{1 - C_o^+}{1 - C^+}\right] = \frac{(TF + TFS)}{V} t \qquad (9)$$

If we let (TF + TFS) be represented by SUM, i.e., TF + TFS = SUM equation (9) reduces to:

$$\ell n \left[\frac{1 - C_o^+}{1 - C^+}\right] = \frac{SUM}{V} t \quad .$$

If we let

$$\ell n \left[\frac{1 - C_o^+}{1 - C^+}\right] = Y \quad ,$$

then

$$Y = \frac{SUM}{V} t \quad . \qquad (10)$$

Equation (10) tells us that a plot of Y versus t should result in a straight line on rectilinear graph paper with a slope equal to $\frac{SUM}{V}$.

If the experiment is run, such that there are no bubbles present in the control volume, the TF term drops out of equation (9). Equation (10) then reduces to:

$$Y = \frac{TFS}{V} t \qquad (10a)$$

Equation (10a) tells us that a plot of Y versus t, in this case, is also a straight line, having a slope equal to $\frac{TFS}{V}$. Hence, one can easily obtain SUM and TFS. TF can then be solved by

$$TF = SUM - TFS \ .$$

The transfer factor is a mass transfer term, which is characteristic of the bubble swarm.

The ultimate goal of this project shall be to find how the Weber number and the Reynolds number affect the transfer factor for the absorption of ammonia by water. Recall that Lin and Donnelly (9) found the Weber number and Reynolds number to be adequate in describing bubble formation and Hauxwell (5) successfully correlated his mass transfer studies from bubbles using these two dimensionless numbers.

EXPERIMENTAL EQUIPMENT AND PROCEDURE

General Considerations

Gas absorption in liquids is usually accompanied by heat effects and volume changes. In the absorption of slightly soluble gases such as oxygen and nitrogen in water, these heat effects and volume changes are negligible. But in the absorption of ammonia in water, the increase in both temperature and volume of the liquid is very large. Since the model presented in the theoretical analysis section involved the recycling of the discharge stream, it is clear that with time, the volume of the liquid in the control volume will increase considerably as ammonia is absorbed. This will violate the assumption that the control volume was constant. In order to overcome this obstacle, the concentration of the ammonia solution in the control volume will be restricted to the dilute range.

The experiment was run at an isothermal temperature of 21.1°C ± 1.5°C and the pressure of the gas in the vapor space above the liquid was maintained at 770 mm Hg. This value of 770 mm Hg was chosen to help avoid the daily changes that occur in the atmospheric pressure. The recycled stream was passed through a heat exchanger to remove any heat of reactions.

The proposed models also included the assumption that the tank was perfectly mixed. Hauxwell (5) used this same tank for his experiment. He did some tracer studies to test the assumption of perfect mixing. He found that the tracer curves obtained were slightly below those that would be obtained if the tank were per-

fectly mixed. This led him to believe that some by-passing of the absorption pool must have occurred. Hence, it was necessary to employ a spatial sampling technique. The actual concentration obtained from his experimental results, using the spatial sampling points indicated, that the assumption of perfect mixing was justified.

Jet nozzles of different diameters were used in this study and hence the construction of the jet nozzle attachment accessories incorporated a degree of flexibility that allowed the interchanging of jet nozzles with little disruption to the rest of the system. Corrosion was minimized by excluding materials, such as brass, which is readily attacked by ammonia.

Since the gas absorption was carried out at an isothermal temperature of 21.1 ± 1.5°C, it was necessary to provide the gas for the absorption studies at 21.1°C. Prior to flowing into the tank, the gas was bubbled into two water pools; this assured that the gas was saturated with water vapor.

Description of Experimental Equipment

A schematic diagram of the equipment is illustrated in Figure 1 and the absorption pool is illustrated in Figure 2. The absorption tank was built by sandwiching a 420 mm I.D. cylindrical glass, about 380 mm high, between two 12.7 mm thick, plexiglass sheets. Holes leading directly into the absorption pool were drilled through the top plexiglass sheet to permit introduction of the gas inlet lines, gas outlet line and the plunging liquid jet nozzle. The bottom

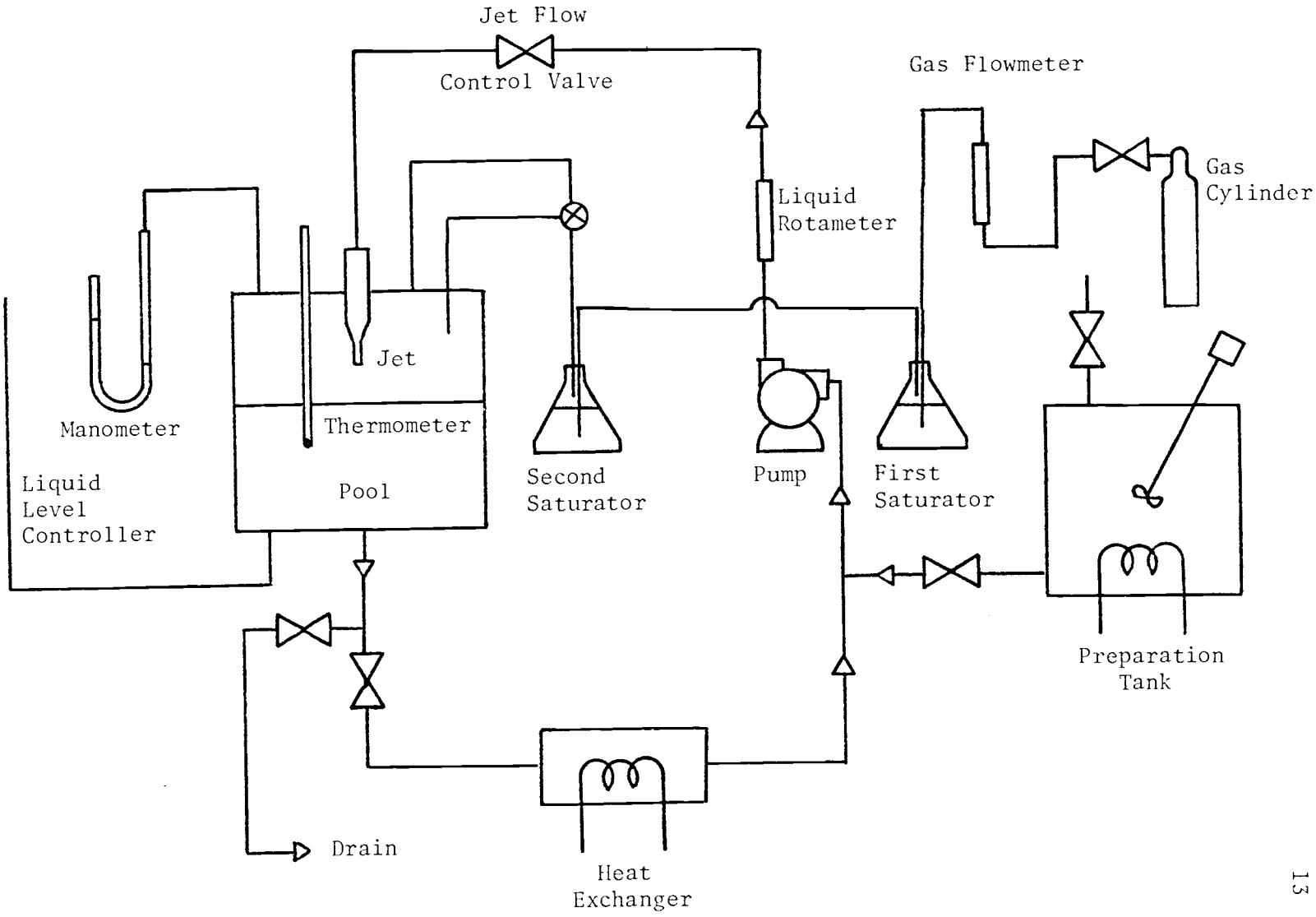

FIGURE 1. SCHEMATIC DIAGRAM OF EQUIPMENT

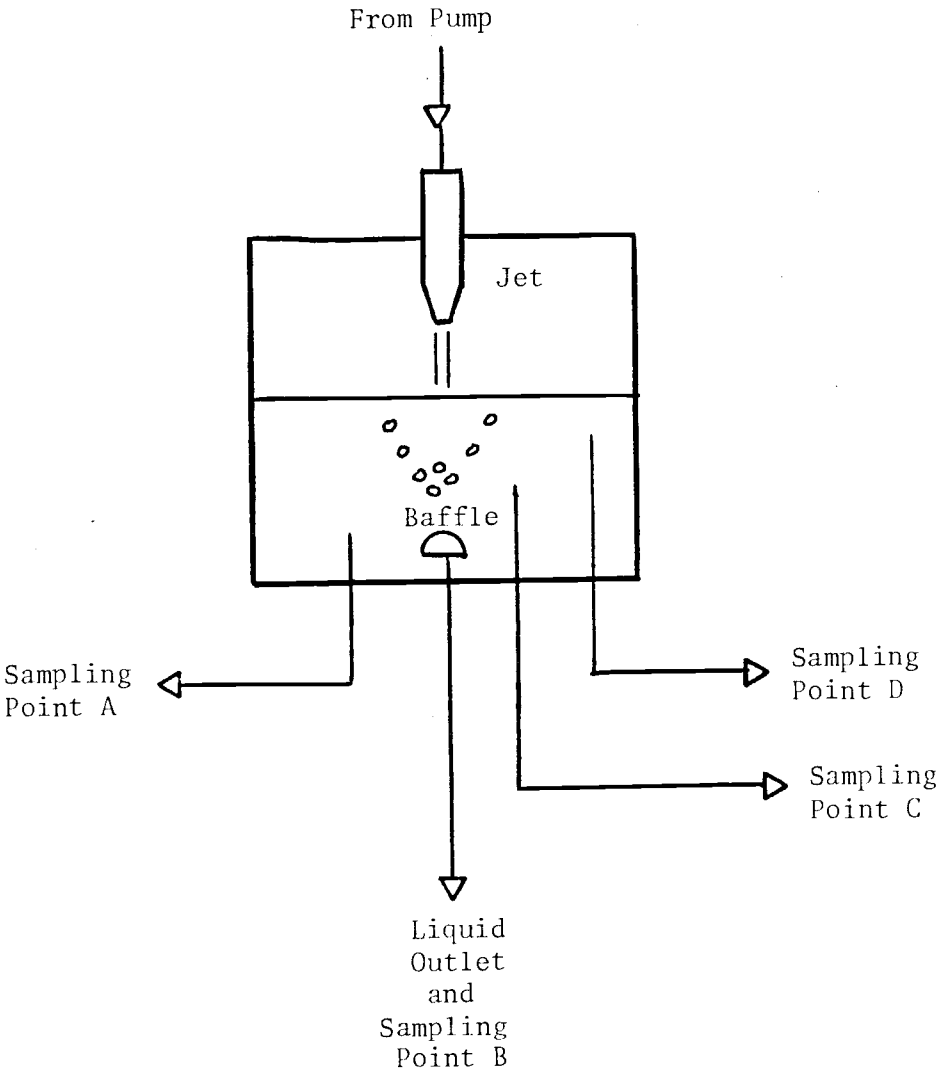

FIGURE 2. ABSORPTION POOL

plexiglass sheet had holes for the water discharge line and the liquid level controller. The liquid level controller consisted of a 1/2-inch O.D. polyethylene tubing that was attached to one of the bottom holes. It could be raised or lowered as desired, and was used in monitoring the level of the liquid in the tank. The bottom sheet also had 3-1/8-inch O.D. stainless steel tubes running through it at radii of 51 mm, 102 mm and 154 mm. These sampling tubes were located 57 mm, 146 mm and 216 mm above the absorption pool bottom. The fourth 1/8-inch O.D. stainless steel sampling point was located in the liquid discharge line, about 13 mm below the bottom of the absorption pool. A metal disk about 40 mm in diameter was anchored at the pool discharge point about 50 mm above the absorption pool bottom. The disk was supported by three wire columns. Hence, any liquid impinging on it from the plunging jet were deflected to the sides. Liquid leaving the absorption pool via the liquid discharge line were not hindered. This baffle helped to improve mixing in the tank by preventing pool by-pass.

The gas line was constructed using 3/8-inch O.D. polyethylene tubing. The gas issuing from the gas cylinder was routed through a flowmeter before bubbling through two 1.8 liter flasks in series that contained pure water initially. The water in the flasks was subsequently saturated with ammonia as was required for the experimental run conditions. The second flask was equipped with a thermometer so that the temperature of the fluid inside could be monitored. The temperature of the fluid inside this second flask was

maintained at 21.1 ± 0.5°C. The second flask was also equipped with an extra tubing so that the saturated liquid could be removed and analyzed for its compsoition. After leaving the saturators, the gas was routed to one of two polyethylene tubings using a tee connection. Both tubes led directly into the absorption pool. One of the tubes was 1/4-inch O.D., while the other was 3/8-inch O.D. The 1/4-inch O.D. tubing was connected to the top of the tank. The 1/4-inch O.D. tubing introduced the gas into the liquid in such a way that the issuing gas was perpendicular to the liquid surface. The 3/8-inch O.D. tubing was connected to the top plexiglass via stainless steel fittings which were screwed into the plexiglass. An L-shaped stainless steel tube about 38 mm by 6 mm was welded to the bottom part of the stainless steel fitting where the gas would have discharged into the pool. The L-shaped part was there to make sure that the gas was introduced parallel to the liquid surface. Since during data acquisition, the gas was introduced into the pool via the 3/8-inch O.D. tubing, it is clear that by introducing the gas into the vapor space horizontal to the liquid surface ensures that no absorption term will arise due to the ammonia gas impinging on the liquid surface directly as opposed to ammonia diffusing to the liquid surface as used in modeling the physical phenomena. Both the 1/4-inch O.D. and the 3/8-inch O.D. tubings were fitted with valves. The gas in the vapor space of the tank had an exit line made of 3/8-inch O.D. polyethylene tubing. One end of the exit line was connected to the vapor space via the

top plexiglass sheet and the other end was connected to a manometer. The absolute pressure of the gas in the vapor space was equal to the atmospheric pressure plus pressure due to the height of liquid displaced in the manometer. The manometer liquid was water. By controlling the flow rate of gas going into the absorption pool, it was possible to control the pressure in the vapor space above the liquid.

The path followed by the liquid used in the absorption studies was such that after the liquid left the high pressure side of the pump, it was routed through a calibrated rotameter located in the 1/2-inch O.D. polyethylene tubing. The liquid then plunged into the control volume via a jet nozzle. The plunging liquid was perpendicular to the surface of the liquid in the absorption tank. If the jet nozzle was above the liquid surface, bubble entrainment phenomena was observed. If it was below the liquid surface, no bubbles were entrained. The liquid in the pool flowed out through 1/2-inch polyethylene discharge line, through a heat exchanger to assure the recycled liquid remained at 21.1°C. The liquid then flowed to the low pressure side of the pump where it was subsequently returned to the pool. A 1/2-inch O.D. polyethylene tube was connected by a tee fitting to the discharge line just below the absorption pool. This line which led directly to the drain system was used in draining the absorption pool, whenever desired. Three jet nozzle of internal diameters: 2.25 mm, 5.40 mm and 6.80 mm were used in the studies. The ratio of the tube length to tube

diameter was such that the velocity profile of the plunging liquid was fully developed prior to plunging into the liquid surface.

Table 1

Nozzle Diameter	Tube Length/Tube Diameter
2.25 mm	136
5.40 mm	92
6.80 mm	64

The plunging liquid stream remained coherent prior to impact.

Experimental Procedure

The water used in the experiment was obtained from a 200 gallon tank which was equipped with an electrical heater and cooling coil tubes. City water was used as initial feed to this preparation tank and the temperature of the water in the tank was maintained at 21.1 ± 1°C.

At the beginning of any run, the appropriate jet nozzle was installed. The nozzle was positioned in the lowest one inch above the 40 liter marking on the absorption tank when bubble entrainment was being investigated and the tip was one-half inch below the 40 liter marking on the absorption tank for absorption through the surface. The inlet tubing to the pump on the low pressure side of the pump was then disconnected from the rest of the system and connected to the preparation tank. The rubber stopper with the 1/4-inch O.D. tubing and the thermometer was removed from the

top plexiglass and replaced by another stopper with a 1/4-inch O.D. tube through it. The other end of this 1/4-inch O.D. tubing was placed under a hood that had a vacuum system. The pump was then started and the water slowly filled the tank. The gas displaced by the water was forced out through the 1/4-inch tube into the hood. The gas was mostly pure air if it was the first run of the day or air-ammonia mixture if it was not. The water was allowed to flow in until it touched the surface of the top plexiglass sheet. By this procedure, all of the gas was eliminated from the absorption tank. The rubber stopper with the 1/4-inch O.D. tubing that directed the evacuated gas to the hood was then replaced with the stopper containing the thermometer and the 1/4-inch O.D. line. The pump inlet tube was then disconnected from the preparation tank and reconnected to the absorption pool discharge line. The absorption system was now in the recycle mode. The saturated ammonia gas was now allowed to flow into the absorption tank via the 1/4-inch O.D. line. Simultaneously, the valve of the draining line was opened so that water from the absorption tank flowed into the building drain system. The vacuum created by the discharging water was immediately filled with the saturated ammonia. The draining process was continued until the liquid level fell below the L-shaped gas inlet tube protruding about 38 mm into the absorption tank. The gas inlet channel was then switched to 3/8-inch O.D. tubing with the help of the three-way valve. When the liquid level approached to within 1000 ml of the 40,000 ml volume that was

used in the experiment, the pump was started and the draining continued until the 40,000 ml mark was reached. The draining process took about 8 minutes. Samples were collected whenever desired in small test tubes. Each test tube could hold up to 10 ml of sample. The samples were obtained from the four, 1/8-inch O.D. stainless steel tubes which have been labeled A, B, C, and D as shown in Figure 2. A sampling technique developed by Hauxwell (5), in which samples from the four sampling locations were "grabbed" simultaneously, was employed here. Prior to obtaining the sample, each test tube was drained of any residual liquid. The bottom of the test tube was then pushed against the bottom of the 1/8-inch O.D. sampling tube. The liquid was allowed to overflow two test tubes volume. It was then tightly stoppered, using a serum cap. When the first set of samples was obtained, time was set equal to zero. The run times were usually short and the ammonia was immediately analyzed for its composition at the end of the run.

Experimental Analysis

Two methods were considered for analyzing the composition of ammonia in solution, namely:

a) Nessler's Method

b) Kjeldahl's Method .

The Nessler's method of analysis is dependent on the formation of an orange colored complex compound $HgO \cdot Hg(NH_2)I$, when the Nessler's reagent, an alkaline solution of potassium mercuric iodide, K_2HgI_4, reacts with the ammonia. The color range for the

complex compound formed by the reaction of ammonia and the Nessler's reagent goes anywhere from yellow to brown, the particular color being proportional in intensity to the concentration of ammonia present. The concentration of ammonia in solution is then determined by visual comparison with solutions of known concentrations of ammonium chloride to which Nessler's reagent has been added. Calcium and magnesium are precipitated by Nessler's reagent. This would interfere with the analysis for ammonia. To overcome this drawback, a few milliliters of a solution of 50 g of Rochelle salt, $KNaC_4H_4O_6$, dissolved in 100 cc of water is usually added to the sample to hold the calcium and magnesium in solution. Another drawback of this analytical technique is that if the solution contains more than a few milligrams of ammonia per 100 cc of solution, an orange precipitate is formed. Accordingly, the use of this method of analysis in the present experiment would involve diluting virtually all the obtained samples before adding the Nessler reagent. This would increase the possibility for errors.

Visible spectrometric methods also can be employed in analyzing the concentration of ammonia in the range 2-25 ppm, using Nessler's reagent at a wavelength of 580 millimicrons.

The Kjeldahl method was used in determining the composition of ammonia in the experimental runs. It involves neutralizing an ammonia solution of known volume with excess sulfuric acid of known concentration and volume. The remaining excess acid is then neutralized, using sodium hydroxide of known concentration. By

knowing the volume of sodium hydroxide that was required to neutralize the excess sulfuric acid, it was then possible to calculate the concentration of ammonia. See Appendix D for a sample calculation. A calibrated syringe was used in removing 5.26 ml of ammonia solution from the serum capped test tube via its needle. The needle was then introduced below the surface of the sulfuric acid in the titrating flask and the ammonical solution forced out into the acid. This technique helped eliminate any possible loss of ammonia due to its volatility. Methyl Red was used as the indicator in this titration. One drop was added to each titrating flask prior to neutralizing the acidic solution with the sodium hydroxide. The following reaction occurs between the ammonia and sulfuric acid, according to Huheey (6):

$$NH_3 + H_2SO_4 = NH_4^+ + HSO_4^- \ .$$

The reaction between the sodium hydroxide and sulfuric acid is as follows:

$$H_2SO_4 + 2NaOH = Na_2SO_4 + 2H_2O \ .$$

DISCUSSION OF RESULTS

After the experimental data were obtained and the pool concentration calculated for the various exposure times and spatial coordinates, an evaluation of the mixing conditions within the tank was made to check the assumption that it was perfectly mixed. The calculated absorption pool concentrations for the various experimental runs are listed in Appendix C with the mean and standard deviation for each set of samples. As can be seen, for all practical purposes, the assumption of perfect mixing was correct.

The next thing that was done was to test the mass transfer model developed in the Theoritcal Analysis section which predicted a straight line when $\ell n \left[\frac{1 - C_o^+}{1 - C^+}\right]$ is plotted against time. The slope of this line is equal to SUM when bubbles are entrained, and equal to TFS when no bubbles are entrained. The dimensionless concentration C^+ is equal to the calculated absorption pool concentration divided by the value of the saturated ammonia solution at the experimental run conditions. An equilibrium concentration value which was determined experimentally to be $17.56 \pm 0.15 \frac{\text{g moles}}{\text{liter}}$ was used. This value compares very favorably with a value of $17.53 \frac{\text{g moles}}{\text{liter}}$ which was calculated, using data reported in the literature. The C_o^+ is the mean of the four sampled pool concentration at time equal to zero divided by $17.56 \frac{\text{g moles}}{\text{liter}}$. Using the procedure as outlined in Appendix D, the value for TFS and

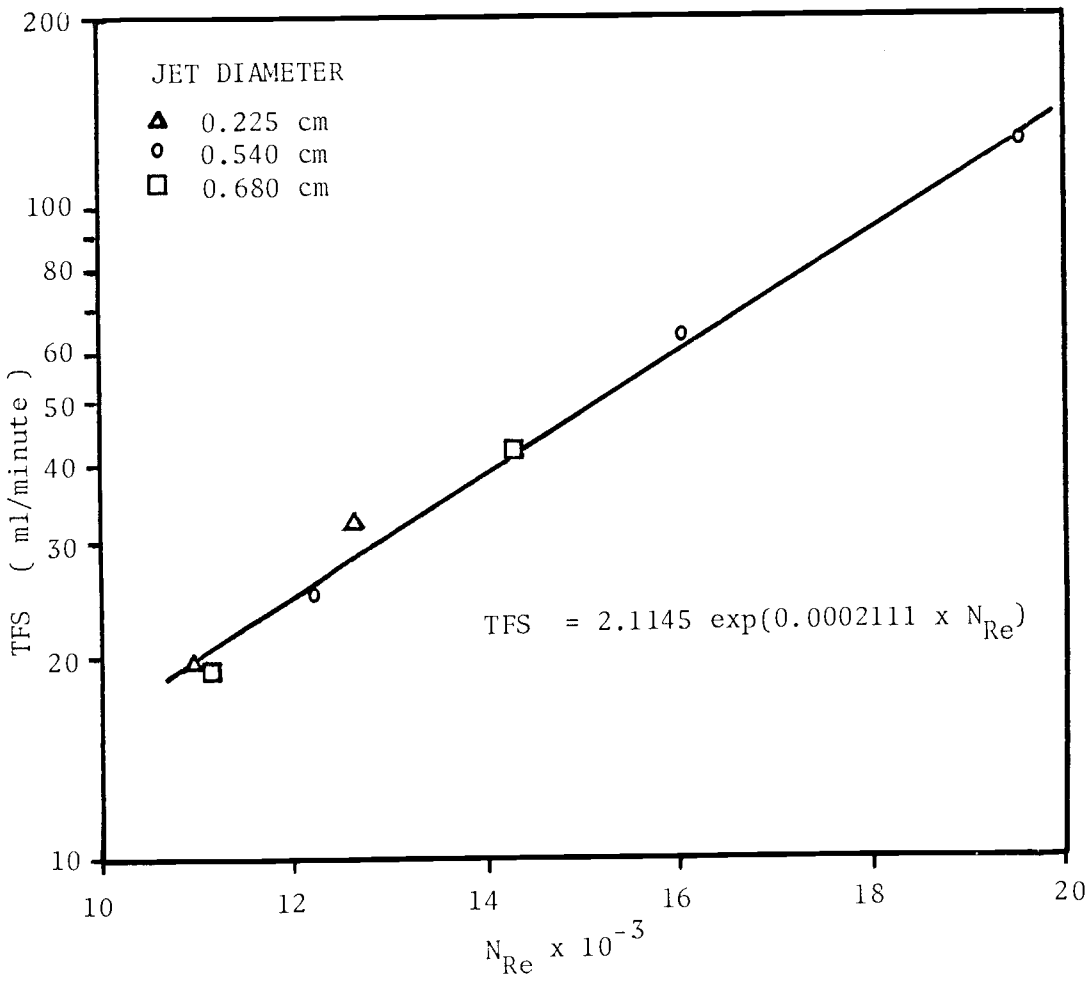

FIGURE 3. SURFACE ABSORPTION COEFFICIENT FOR AMMONIA

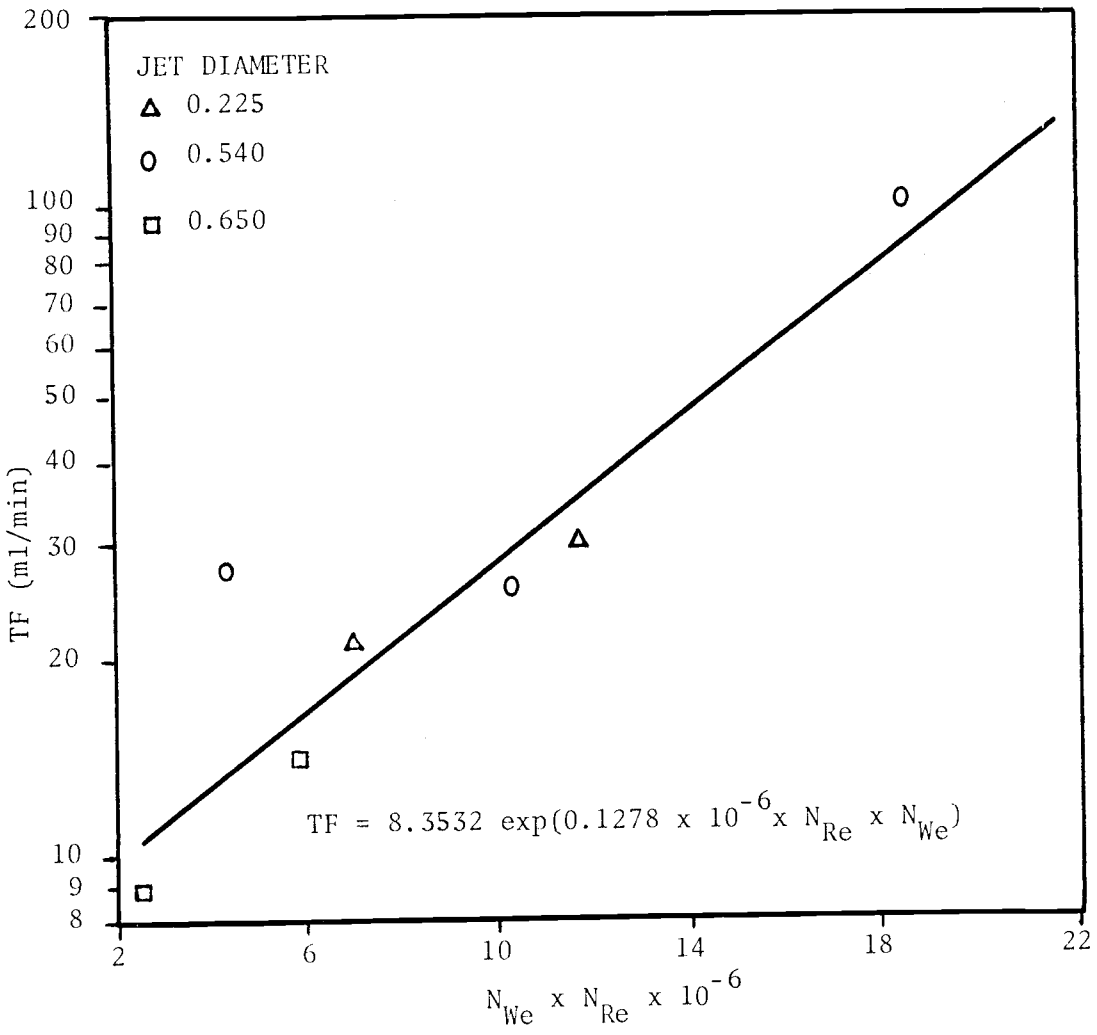

FIGURE 4. TRANSFER FACTOR FOR AMMONIA

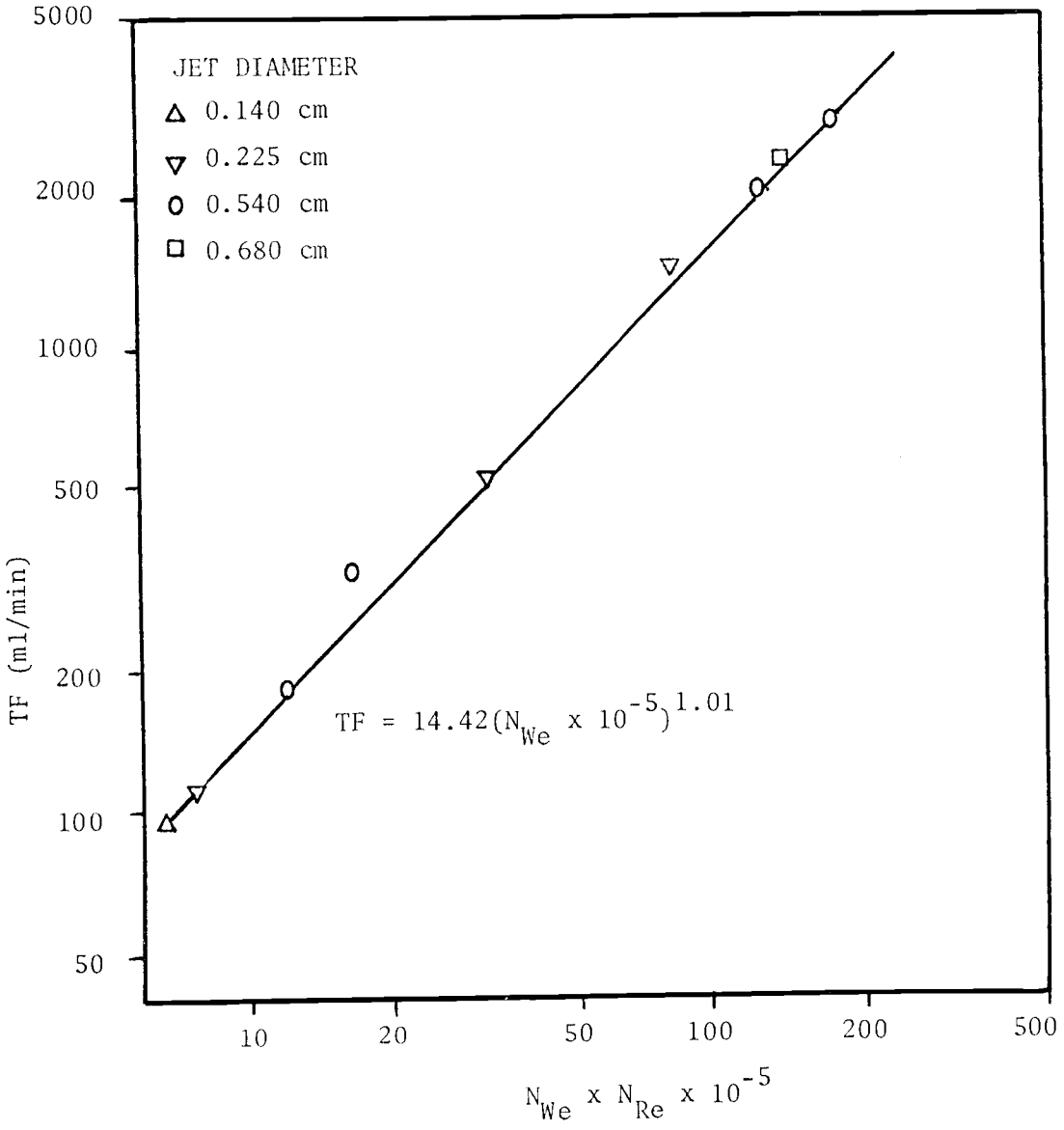

FIGURE 5. TRANSFER FACTOR FOR OXYGEN*

*Data of Hauxwell(5)

SUM were obtained using the least square fit. The 95% confidence limits for SUM and TFS along with their correlation coefficients are listed in Appendix C. Recall from equation (10),

$$SUM = TFS + TF \tag{10}$$

It was possible to calculate TF using the experimental SUM and TFS values. The calculated values of TF along with the 95% confidence limits are listed in Appendix C.

The values of TFS for various jet diameters employed was successfully correlated with the jet stream Reynolds number. The analysis technique employed forced the data to a straight line. In going from a jet stream Reynolds number of 11,000 to 16,000, the TFS increased from 21 $\frac{ml}{min}$ to 65 $\frac{ml}{min}$ or an increase of 209.5%.

The TF values were correlated with the product of the jet stream Reynolds number and the Weber number, ($N_{Re} \times N_{We}$); the product of two dimensionless number is equivalent to the rate at which the jet stream supplies kinetic energy to the pool. The correlation for TF as a function of the product of the jet stream Reynolds number and Weber number gives a nice linear fit. The only data points which seems to deviate from this general observation, is that obtained from Run No. 0.540-12276-0-S and Run No. 0.540-12226-366-B. The transfer factor, TF, obtained here was larger than expected. Since the experimental surface transfer value for Run No. 0.540-12226-0-S was essentially the same as predicted by its correlating equation, the source of the discrepancy in the TF value was due to the evaluation of its SUM value.

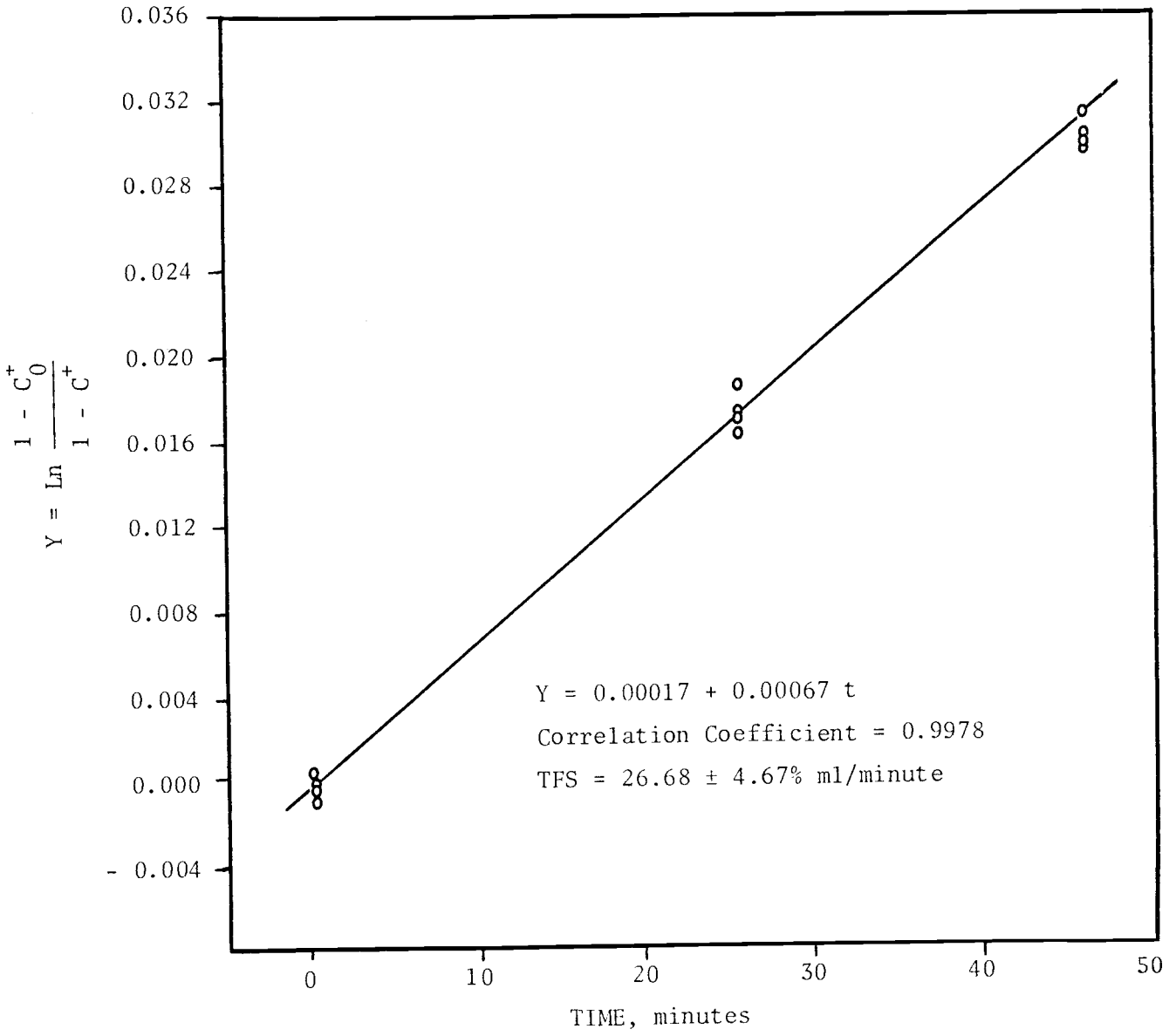

FIGURE 6. DETERMINATION OF TFS FOR RUN NO. 0.540-12226-0-S

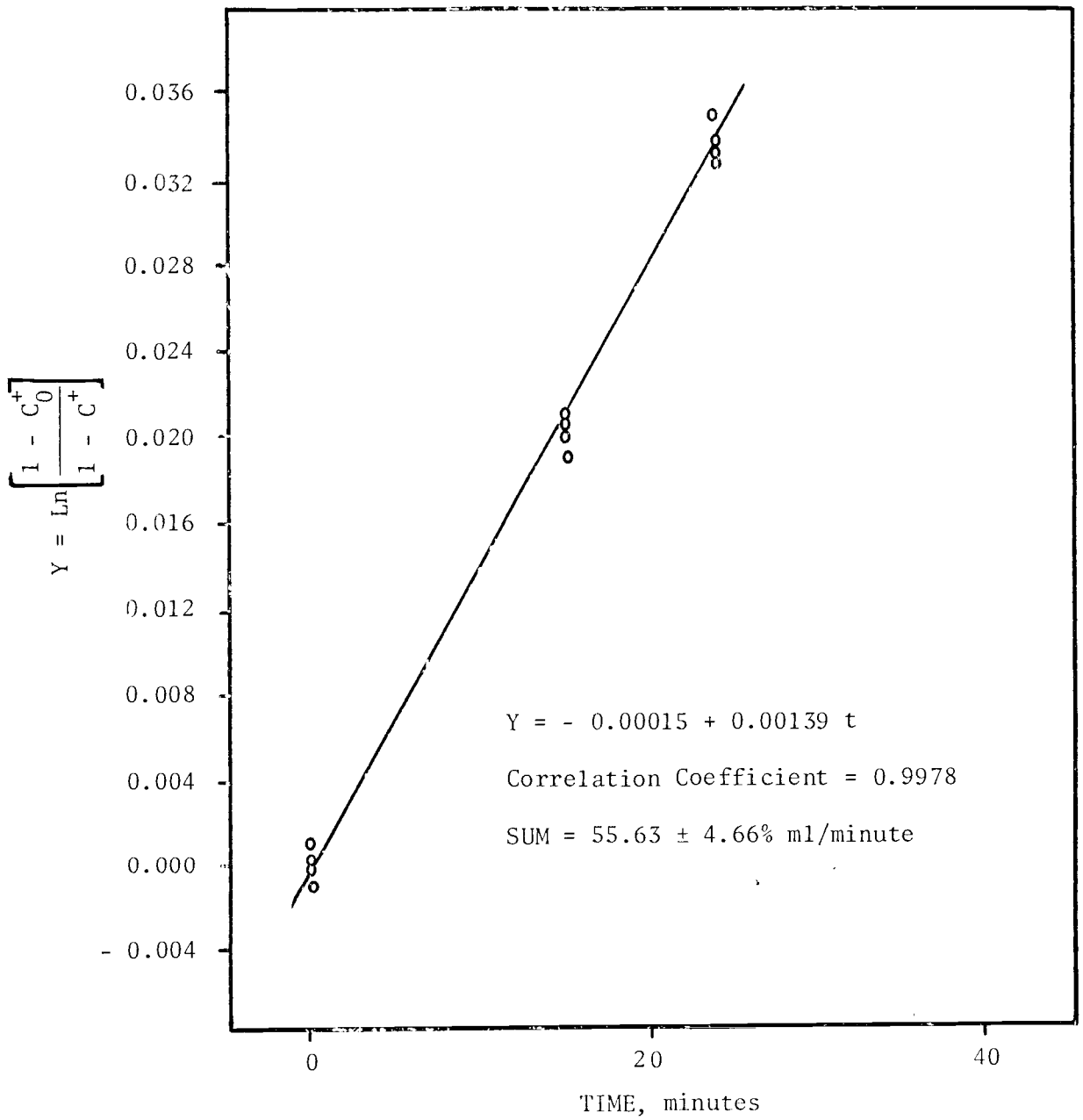

FIGURE 7. DETERMINATION OF SUM FOR RUN NO. 0.540-12226-366-B

A brief review of the data of Lin and Donnelly (9) might help shed some light on this unexpected observation. In their experimental investigation, they noted:

a) The bubble diameters decrease at higher flowrates; and

b) While the bubble formation frequency increases at higher flowrates, the ratio of the bubble entrainment (cc/sec) to that of liquid flowrate (cc/sec), increase only moderately with increasing flowrates.

The two things that might be expected to yield a high TF value would be bubbles with a large surface area, this would mean large diameters and a high rate of entrainment per liquid flowrate, assuming the TFS value remains unchanged. For the range of values covered, Run No. 0.540-12226-366-B had the third lowest flowrate. For the seven products of Reynolds number and Weber number tabulated, it also has the second lowest value. Thus the possibility of obtaining a higher TF value than expected at the prevailing condition should not come as a total surprise.

The present experiment will be compared to that of Hauxwell (5) for purposes of comparing the magnitude of the measured values. In order to accomplish this, experimental values obtained from similar dynamic conditions were used. The TF value obtained from Run No. 0.540-19643-944-B, is 103.03 $\frac{ml}{min}$. For the oxygen absorption studies of Hauxwell (5), the corresponding TF value, at the same value of $N_{Re} \times N_{We}$, is 2857 $\frac{ml}{min}$. The diffusivity of ammonia in

liquid water and that of oxygen in liquid water are listed in Appendix C. The ratio of $D_{O_2-H_2O}$ to $D_{NH_3-H_2O}$ is 1.40. Obviously the magnitude of the diffusivities cannot be the only factor which produce such a wide difference in the magnitude of the transfer factor, TF.

In order to understand why these values of TF differ, some aspects of mass transfer at the gas-liquid interface will be reviewed. The total resistance to mass transfer across a gas-liquid interface lies in the individual film resistance: gas film resistance and liquid film resistance. By electrical analogy, we have:

$$\frac{1}{K_L} = \frac{1}{k_L} + \frac{1}{Hk_a} \tag{11}$$

K_L = overall mass transfer coefficient

k_L = liquid film mass transfer coefficient

k_G = gas film mass transfer coefficient

H = Henry's law constant

If equation (11) is multiplied by the reciprocal of the interfacial area of the bubble and summed over all the bubbles, this would result in:

$$\frac{1}{K_L A} = \frac{1}{TF} = \frac{1}{k_L A} + \frac{1}{Hk_G A} \tag{12}$$

Note that TF in equation (12) was experimentally determined for Run No. 0.540-19643-944-B to be 103.03 $\frac{ml}{min}$. King (8) has discussed the limitations of equation (12). These limitations include:

a) H must be constant or if it is not, the value of the equilibrium slope at the concentration (equilibrium) must be used.

b) No interfacial resistance. In other words, equilibrium exists at the gas-liquid interface.

c) The mass transfer resistance of the two phases must not interact; that is the magnitude of k_L at any point must be independent of k_G.

d) The ratio of $\frac{Hk_G}{k_L}$ must be constant at all points on the interface.

While in this project, all the limitations on equation (12) are not claimed to have been met, equation (12) can still serve as a useful tool in the present analysis. Previous correlation for evaluating the mass transfer coefficient have shown that each film mass transfer coefficient is a product of some function of the Reynolds number and some function of the diffusivity. Several theories have been proposed to explain how the film mass transfer coefficient varies with the diffusivity. For example, the Whitman's two film theory proposes that the film mass transfer coefficient varies with the diffusivity to the power of one and the surface renewal or penetration theory proposed that the film mass transfer coefficient varies with the diffusivity to the power of one-half.

If the experiments with the oxygen (solute gas) and ammonia (solute gas) are run at identical flow conditions, the ratio of

the equations for each particular phase, i.e., gas or liquid phase, permit the canceling of the turbulence function, yielding:

a) with the Whitman's two-film model:

$$\frac{(k_L A)_{NH_3}}{(k_L A)_{O_2}} = \left(\frac{D_{NH_3\text{-}H_2O}}{D_{O_2\text{-}H_2O}}\right)_{\text{liquid}} \tag{13}$$

$$\frac{(k_G A)_{NH_3}}{(k_G A)_{O_2}} = \left(\frac{D_{NH_3\text{-}H_2O}}{D_{O_2\text{-}H_2O}}\right)_{\text{vapour}}^{\text{vapour}} \tag{14}$$

and

b) with the surface renewal or penetration model:

$$\frac{(k_L A)_{NH_3}}{(k_L A)_{O_2}} = \left[\left(\frac{D_{NH_3\text{-}H_2O}}{D_{O_2\text{-}H_2O}}\right)_{\text{liquid}}\right]^{1/2} \tag{15}$$

$$\frac{(k_G A)_{NH_3}}{(k_G A)_{O_2}} = \left[\frac{D_{NH_3\text{-}H_2O}}{D_{O_2\text{-}H_2O}}^{\text{vapour}}_{\text{vapour}}\right]^{1/2} \tag{16}$$

Substituting known (experimental) values of $(TF)_{NH_3}$ and $(TF)_{O_2}$ in equation (12) will yield two equations. These two equations along with equations (13) and (14) or equation (15) and (16), depending on the mass transfer model that is assumed, yield four equations with four unknowns. In this way, the four film mass transfer coefficients can be evaluated using the value of H found in Appendix D. The individual film mass transfer coefficients are tabulated on the next page.

Table 2. Individual Film Transfer Factor for Run No. 0.540-19643-944-B

Mass Transfer Model	Film Transfer Factor (ml/min) ammonia liquid k_LA	ammonia gas Hk_GA	oxygen liquid k_LA	oxygen gas Hk_GA
Whitman's two-film model	2054.65	108.64	2881.65	1.198×10^6
Surface Renewal or Penetration Model	2417.8	107.61	2864.6	1.287×10^6

Note that k_GA had to be multiplied by H for the units to be consistent, ml/min. The fraction of gas film resistance to the total resistance is the reciprocal of H x k_GA to the reciprocal of the transfer factor. The calculated values are listed in Table 3.

Table 3. Fraction of Total Resistance Contributed by the Gas Film for Run No. 0.540-19643-944-B and Dynamically Similar Hauxwell Oxygen Absorption Data

Mass Transfer Model	Percentage Resistance in Gas Film Ammonia	Oxygen
Whitman's two-film model	94.98%	0.259%
Surface renewal or penetration model	95.74%	0.257%

The gas film resistances tabulated in Table 3 are significant, in that they help to explain the big difference in the magnitude of the TF values for ammonia and oxygen. To illustrate this, the Whitman film model will be used; however, this approach is equally applicable to the surface renewal or penentration model.

For Run No. 0.540-19643-944-B:

$(k_L A)_{NH_3} = 2054.65$ $\qquad$ $(k_L A)_{O_2} = 2881.65$

$(k_G A)_{NH_3} = 1.93$ $\qquad$ $(k_G A)_{O_2} = 1.64$

These values are for the Whitman two-film model. As can be seen, the variations when the values for ammonia are compared with that for oxygen is indeed minor compared to the difference between $(TF)_{O_2}$ and $(TF)_{NH_3}$. The answer lies in the Henry's law constant, H. The H for oxygen is 730,360 while the H for ammonia is 56.29. Thus the value of H has a tremendous impact on the gas phase resistance.

Hauxwell (5) noted that carbon dioxide was about 40 times more soluble than oxygen in water. The values of $(TF)_{CO_2}$ were about one-third those of $(TF)_{O_2}$. For the present system of ammonia-water, ammonia is 12,975 times more soluble in water than oxygen. However the transfer factor, TF, for Run No. 0.540-19643-944-B is only 0.036 times the TF for oxygen. Thus the effect of solubility on the transfer factor is significant and should not be ignored.

CONCLUSION

1. The transfer factor, which is the product of the interfacial area and the overall liquid mass transfer coefficient summed over all the entrained bubbles, was experimentally determined for the ammonia-water system in the dilute range. The mathematical models developed to yield values of TFS and SUM for subsequent determination of TF, correlated the experimental values well. The jet stream Reynolds number varied from 10,887 to 19,643 while the jet stream Weber number varied from 233 to 944. Three different jets of diameters 0.225 cm, 0.540 cm and 0.680 cm were used.
2. The transfer factor was successfully correlated using the product of the jet stream Reynolds number and Weber number. The product of these two dimensionless numbers is the rate at which the jet stream is suppling kinetic energy to the absorption pool.
3. The solubility of the gas was found to have a profound effect on the TF value obtained. The transfer factor is an inverse function of the solubility. Ammonia is 12,975 times more soluble than oxygen in water if the partial pressure of the gas is about 752 mm Hg and the water is at 70°F and 1 atmosphere. The $(TF)_{NH_3}$ obtained from Run No. 0.540-19643-944-B was found to be 0.036 times the $(TF)_{O_2}$.

NOMENCLATURE

A	-	Interfacial area
C	-	Concentration of solute gas
C*	-	Equilibrium concentration of solute gas
C+	-	Dimensionless ratio, C/C*
D_{ij}	-	Molecular diffusivity
D_j	-	Jet diameter
d.f.s	-	Degrees of freedom for TFS
d.f.b	-	Degrees of freedom for SUM
d.f.c	-	Approximate degrees of freedom in determining TF
g_c	-	Newton's law conversion factor 980.665 ($gM_M cm/gM_f sec^2$)
H	-	Henry's law constant
k_G	-	Gas film mass transfer coefficient
k_L	-	Liquid film mass transfer coefficient
K_L	-	Overall liquid mass transfer coefficient
N_{Re}	-	Jet stream Reynolds number ($D_j V/\mu_l$)
N_{We}	-	Jet stream Weber number ($DjV^2\rho/\sigma g_c$)
N	-	Units of concentration, (Normality), $\frac{\text{equivalents}}{\text{liter}}$
R	-	Rate of gas absorption
SUM	-	TF + TFS
TF	-	Transfer factor
TFS	-	Surface transfer factor
V	-	Average velocity of jet stream
s	-	Standard deviation

μ - Mean

μ_l - Viscosity

σ - Surface tension

ρ - Density

BIBLIOGRAPHY

1. Calderbank, P. H. Physical rate processes in industrial fermentation. Part II. Mass transfer coefficients in gas-liquid contacting with and without mechanical agitation. 1959. Trans. Instn. Chem. Eng. 37, 173-185.

2. Chiang, S. H. and Toor, H. L. Gas absorption accompanied by large heat effects and volume change of the liquid phase. 1964. A.I.Ch.E. Journal. 10:398-402.

3. Fritz, J. S. and Schenk, G. H. Quantitative analytical chemistry. 1974. Boston, Allyn and Bacon. 689 pp.

4. Furman, N. H. Scott's standard method of chemical analysis. 1939. 5th ed., Vol. 1. D. Van Nostrand. 1234 pp.

5. Hauxwell, G. D. Pool absorption of gas entrained by plunging liquid jet. 1972. Ph.D. Thesis. Corvallis, Oregon State University.

6. Huheey, J. E. Inorganic chemistry: Principles of structure and reactivity. 1972. New York, Harper and Row. 737 pp.

7. Jackson, L. M. Aeration in Bernoulli type devices. 1964. A.I.Ch.E. Journal. 10:836-842.

8. King, J. C. The additivity of individual phase resistances in mass transfer operation. 1964. A.I.Ch.E. Journal. 10:671-676.

9. Lin, T. J. and Donnelly, H. G. Gas bubble entrainment by plunging laminar liquid jets. 1966. A.I.Ch.E. Journal. 12:563-571.

10. Miller, I. and Freund, J. E. Probability and statistics for engineers. 1965. Englewood Cliffs, Prentice-Hall, 432 pp.

11. Perry, R. H. and Kirkpatrick, S. D. Chemical engineers handbook. 1963. 4th ed. New York, McGraw-Hill.

12. Reid, R. C. and Sherwood, T. K. The properties of gases and liquids. 1966. New York, McGraw-Hill. 646 pp.

13. Snell, F. D. and Biffen, F. M. Commercial method of analysis. 1944. New York, McGraw-Hill. 753 pp.

14. Swiggett, G. E. Gas absorption by entrainment from a plunging liquid jet. 1968. Ph.D. Thesis. Corvallis, Oregon State University. 103 pp.

15. Treybal, R. E. Mass transfer operation. 1968. New York, McGraw-Hill. 717 pp.

16. Washburn, E. W. International critical tables. 1928. New York, McGraw-Hill. 444 pp.

17. Welcher, F. J. Standard methods of chemical analysis. 1966. 6th ed., Vol. 3, part A. Princeton, D. Van Nostrand. 974 pp.

18. Yoe, J. H. Photometric chemical analysis. 1928. Vol 1. New York, John Wiley and Sons. 771 pp.

APPENDICES

APPENDIX A

Experimental Code

Each run was coded as follows:

XXXX —— YYYYY —— ZZZ —— P

XXXX = Jet diameter in centimeters

YYYYY = Jet stream Reynolds number, N_{Re}

ZZZ = Jet stream Weber number, N_{We}

P = Purpose of the run

If P = S, Surface absorption

If P = B, Bubble and surface absorption

APPENDIX B

Equipment and Material Specification

Table B-1. Pool Volume Calibration*

Pool Depth, d (mm)	Volume, V (liters)
25.4	3.110
28.6	3.500
55.6	7.368
79.4	11.126
106.4	15.017
128.6	18.588
152.4	22.117
176.2	25.784
200.0	29.322
223.8	32.957
247.6	36.658
269.9	40.202

$$V(\text{liters}) = -0.9316 + 0.1517\ d(\text{mm})$$

* Data of Hauxwell (5). This pool volume calibration was verified prior to the experimental runs.

Table B-2. Gear Pump

Mfgr.:	Leland Electric Co.
Serial #1:	P 114 BB
Motor Size:	1/3 hp

Table B-3. Reagent Specification

1. Ammonia Gas:

   Anhydrous ammonia (Refrigeration Grade)

2. Sodium Hydroxide:

   Sodium hydroxide pellets. 97.3% pure; (Baker analyzed reagent)

3. Sulfuric Acid:

   Sulfuric acid. 96.5% pure; (Baker analyzed reagent)

Table B-4. Calibration of Rotameter (Fisher and Porter with tube No. B5-27-10/70G)

Meter Indication	Flow Rate (liter/min)
59	5.886
59	5.843
59	5.855
50	5.018
50	5.017
50	5.012
40	4.053
40	4.068
30	3.048
30	3.031
25	2.545
25	2.611
20	2.076
20	2.070
20	2.080
10	1.082
10	1.102

APPENDIX C

Experimenta Data

Table C-1. Precision of Syringe Volume

Sample No.	Weight of Water Sample (gm)
1	5.2598
2	5.2599
3	5.2601
4	5.2602
5	5.2601
6	5.2599

Average = 5.2600

S = 0

Table C-2. Physical Properties of Fluids*. Water at 1 Atmosphere

Temperature	Density	Viscosity	Surface Tension	Vapor Pressure	ρ/μ_1	$\rho/\sigma g_c$
^oC	gm/ml	centipoise	dynes/cm	mm/Hg	sec/cm^2	sec^2/cm^3
20.0	0.998	1.0050	72.75	17.52	99.30	0.01372
25.0	0.997	0.8937	71.97	--	111.56	0.01385
30.0	0.9957	0.8007	71.18	31.82	124.35	0.01399
35.0	0.994	0.7225	70.38	--	137.58	0.01412

From interpolation at 21.1^oC

$\rho/\mu_1 = 102.02\ sec/cm^2$

$\rho/\mu g_c = 0.01375\ sec^2/cm^3$

$P_{H_2O} = 18.76$ mm Hg

*Data of Hauxwell

Table C-3. Physical Properties of Fluids

Liquid Diffusivity

System	Temperature °C	D x 10^5 (cm^2/s)	Source
NH_3-H_2O	12	1.64	Experimental Value
	12	1.65	Wilke-Chang Equation
	21.1	1.69	Wilke-Chang Equation
O_2-H_2O	25	2.41	Experimental Value
	25	2.40	Wilke-Chang Equation
	21.1	2.37	Wilke-Chang Equation

Reference: Reid and Sherwood (12)

Table C-4. Physical Properties of Fluids

Gas Diffusivity in Water Vapor

The method of Fuller, Schettler and Giddings is used for the calculations.

$D_{O_2-H_2O}$ (experimental at 79.3°C) = 0.352 cm^2/sec

$D_{O_2-H_2O}$ (calc. Fuller et al. at 79.3°C) = 0.354 cm^2/sec

$D_{O_2-H_2O}$ (calc. Fuller et al. at 21.1°C) = .2582 cm^2/sec

$D_{NH_3-H_2O}$ (calc. Fuller et al. at 21.1°C) = .3038 cm^2/sec

Reference: Reid and Sherwood (12)

Data Acquisition

In all the experimental runs, the volume of liquid used in the absorption studies was 40,008.4 ml. The volume of ammonia solution that was analyzed for its composition in all the experimental runs was 5.26 ml, except in the determination of the equilibrium concentration of the ammonia solution as listed in Appendix C. Thus only 5.26 ml of the solution withdrawn from sample ports A, B, C, and D was analyzed for its composition. The experimental runs have been coded as explained in Appendix A.

Table C-5. Pool concentration for Run No. 0.225-10887-0-5

Concentration of H_2SO_4 = 3.0853 N

Concentration of NaOH = 3.0990 N

Volume of H_2SO_4 used (ml)

Sample Position	Time(min) 0	16	30
A	3.00	3.05	3.00
B	3.00	3.00	3.00
C	3.00	3.00	3.00
D	3.00	3.00	3.00

Volume of NaOH used (ml)

Sample Position	Time(min) 0	16	30
A	2.77	2.55	2.31
B	2.86	2.52	2.35
C	2.82	2.57	2.39
D	2.80	2.52	2.36

Table C-6. Pool concentration for Run No. 0.225-10887-696-B

Concentration of H_2SO_4 = 3.0853 N

Concentration of NaOH = 3.0990 N

Volume of H_2SO_4 used (ml)

Sample Position	Time(min) 0	6	14
A	3.00	3.05	3.40
B	3.05	3.00	3.80
C	2.97	3.00	3.94
D	2.98	3.00	3.94

Volume of NaOH used (ml)

Sample Position	Time(min) 0	6	14
A	2.50	2.39	2.48
B	2.54	2.34	2.80
C	2.45	2.36	3.00
D	2.47	2.35	3.01

Table C-7. Pool concentration for Run No. 0.225-12667-0-S

Concentration of H_2SO_4 = 3.0853 N

Concentration of NaOH = 2.9660 N

Volume of H_2SO_4 used (ml)

Sample Position	Time(min) 0	13	21
A	2.98	3.00	2.90
B	3.06	3.00	3.00
C	3.00	3.00	3.00
D	3.00	3.00	3.00

Volume of NaOH used (ml)

Sample Position	0	13	21
A	2.93	2.52	2.42
B	2.98	2.57	2.37
C	2.94	2.56	2.37
D	2.94	2.56	2.35

Table C-8. Pool concentration for Run No. 0.225-12667-942-B

Concentration of H_2SO_4 = 3.0853 N

Concentration of NaOH = 3.0990 N

Volume of H_2SO_4 used (ml)

Sample Position	Time(min) 0	8.5	16
A	3.00	3.08	3.05
B	3.10	2.95	3.02
C	2.90	3.00	3.03
D	3.15	3.00	3.05

Volume of NaOH used (ml)

Sample Position	0	8.5	16
A	2.82	2.49	2.08
B	2.95	2.36	2.08
C	2.75	2.41	2.09
D	2.98	2.42	2.09

Table C-9. Pool concentration for Run No. 0.540-12226-0-S

Concentration of H_2SO_4 = 3.1226 N

Concentration of NaOH = 3.0990 N

Volume of H_2SO_4 used (ml)

Sample Position	Time(min) 0	25.5	46
A	2.94	3.20	4.69
B	3.17	3.19	4.31
C	3.62	3.46	4.40
D	3.41	3.45	4.35

Volume of NaOH used (ml)

Sample Position	Time(min) 0	25.5	46
A	2.71	2.49	3.36
B	3.02	2.56	3.30
C	3.47	2.80	3.37
D	3.29	2.79	3.31

Table C-10. Pool concentration for Run No. 0.540-12226-366-B

Concentration of H_2SO_4 = 3.1226 N

Concentration of NaOH = 3.0990 N

Volume of H_2SO_4 used (ml)

Sample Position	Time(min) 0	15	24
A	4.72	5.05	4.88
B	4.83	4.98	5.32
C	5.36	4.97	4.79
D	3.77	4.94	5.32

Volume of NaOH used (ml)

Sample Position	Time(min) 0	15	24
A	4.64	4.38	3.85
B	4.81	4.32	4.30
C	5.32	4.32	3.80
D	3.70	4.32	4.25

Table C-11. Pool concentration for Run No. 0.540-16130-0-S

Concentration of H_2SO_4 = 3.1226 N

Concentration of NaOH = 3.0990 N

Volume of H_2SO_4 used (ml)

Sample Position	Time(min) 0	6.5	12
A	3.05	3.25	2.35
B	3.10	3.20	3.41
C	2.89	3.11	3.04
D	3.21	3.28	3.40

Volume of NaOH used (ml)

Sample Position	Time(min) 0	6.5	12
A	2.62	2.53	1.46
B	2.78	2.47	2.49
C	2.49	2.43	2.10
D	2.82	2.59	2.38

Table C-12. Pool concentration for Run No. 0.540-16130-637-B

Concentration of H_2SO_4 = 3.1226 N

Concentration of NaOH = 3.0990 N

Volume of H_2SO_4 used (ml)

Sample Position	Time(min) 0	5	9
A	3.54	3.25	5.20
B	4.01	3.77	4.71
C	3.60	4.48	5.07
D	4.08	3.91	4.57

Volume of NaOH used (ml)

Sample Position	Time(min) 0	5	9
A	3.45	2.81	4.51
B	3.90	3.39	3.99
C	3.50	4.01	4.37
D	3.98	3.49	3.88

Table C-13. Pool concentration for Run No. 0.540-19643-0-S

Concentration of H_2SO_4 = 3.0853 N

Concentration of NaOH = 3.0990 N

Volume of H_2SO_4 used (ml)

Sample Position	Time(min) 0	5	9.5
A	3.00	3.01	4.00
B	3.00	3.00	4.00
C	3.10	3.01	4.00
D	3.01	3.00	4.00

Volume of NaOH used (ml)

Sample Position	Time(min) 0	5	9.5
A	2.30	1.82	2.41
B	2.31	1.82	2.40
C	2.36	1.80	2.40
D	2.30	1.82	2.42

Table C-14. Pool concentration for Run No. 0.540-19643-944-B

Concentration of H_2SO_4 = 3.1226 N

Concentration of NaOH = 3.0990 N

Volume of H_2SO_4 used (ml)

Sample Position	Time(min) 0	3	7.5
A	3.48	4.76	4.13
B	3.64	4.26	4.31
C	3.30	4.57	4.01
D	3.51	4.67	4.35

Volume of NaOH used (ml)

Sample Position	Time(min) 0	3	7.5
A	3.12	3.84	2.48
B	3.28	3.20	2.71
C	2.77	3.77	2.27
D	3.08	3.74	2.64

Table C-15. Pool concentration for Run No. 0.680-10949-0-S

Concentration of H_2SO_4 = 3.0853 N

Concentration of NaOH = 2.9666 N

Volume of H_2SO_4 used (ml)

Sample Position	Time(min) 0	13.5	23
A	2.98	3.00	3.04
B	3.00	3.03	2.99
C	3.10	3.00	3.02
D	3.00	3.00	3.00

Volume of NaOH used (ml)

Sample Position	Time(min) 0	13.5	23
A	3.03	2.85	2.74
B	3.08	2.86	2.72
C	3.20	2.82	2.74
D	3.06	2.82	2.73

Table C-16. Pool concentration for Run No. 0.680-10949-233-B

Concentration of H_2SO_4 = 3.0853 N

Concentration of NaOH = 2.9666 N

Volume of H_2SO_4 used (ml)

Sample Position	Time(min) 0	10	20
A	3.01	3.00	3.00
B	3.01	3.00	3.00
C	3.00	3.00	2.98
D	3.02	2.86	3.00

Volume of NaOH used (ml)

Sample Position	Time(min) 0	10	20
A	2.79	2.40	2.24
B	2.78	2.40	2.29
C	2.80	2.40	2.37
D	2.77	2.26	2.35

Table C-17. Pool concentration for Run No. 0.680-14359-0-S

Concentration of H_2SO_4 = 3.0853 N

Concentration of NaOH = 2.9666 N

Volume of H_2SO_4 used (ml)

Sample Position	Time(min) 0	11	20
A	3.00	2.60	3.00
B	3.00	2.82	3.00
C	3.00	2.68	3.00
D	3.00	3.00	3.00

Volume of NaOH used (ml)

Sample Position	Time(min) 0	11	20
A	2.82	2.05	2.25
B	2.90	2.33	2.23
C	2.86	2.14	2.20
D	2.86	2.51	2.23

Table C-18. Pool concentration for Run No. 0.680-14359-401-B

Concentration of H_2SO_4 = 3.0853 N

Concentration of NaOH = 2.9666 N

Volume of H_2SO_4 used (ml)

Sample Position	Time(min) 0	6	10
A	2.98	3.00	3.00
B	3.00	3.00	3.00
C	3.00	3.00	3.00
D	3.00	3.00	3.00

Volume of NaOH used (ml)

Sample Position	Time(min) 0	6	10
A	2.85	2.62	2.45
B	2.87	2.60	2.43
C	2.88	2.60	2.44
D	2.87	2.58	2.46

Table C-19. Equilibrium concentration determination, C* at 21.1°C and 770 mm Hg

Sample No. 1

Concentration of H_2SO_4 = 3.1226 N

Concentration of NaOH = 3.0990 N

Volume of NH_3 used = 3.80 ml

Volume of H_2SO_4 used = 39.79 ml

Volume of NaOH used = 18.95 ml

Table C-20. Equilibrium concentration determination, C* at 21.1°C and 770 mm Hg

Sample No. 2

Concentration of H_2SO_4 = 3. 1226 N

Concentration of NaOH = 3.0990 N

Volume of NH_3 used = 4.04 ml

Volume of H_2SO_4 used = 29.38 ml

Volume of NaOH used = 6.52 ml

Table C-21. Equilibrium concentration determination, C* at 21.1°C and 770 mm Hg

Sample No. 3

Concentration of H_2SO_4 = 3.0853 N

Concentration of NaOH = 3.0990 N

Volume of NH_3 used = 4.1 ml

Volume of H_2SO_4 used = 29.64 ml

Volume of NaOH used = 6.26 ml

Table C-22. Equilibrium concentration determination, C* at 21.1°C and 770 mm Hg

Sample No. 4

Concentration of H_2SO_4 = 3.0853 N

Concentration of NaOH = 2.9666 N

Volume of NH_3 used = 6.4 ml

Volume of H_2SO_4 = 54.45 ml

Volume of NaOH used = 18.38 ml

Table C-23. Pool concentration for Run No. 0.225-10887-0-S

Concentration in g moles/liter

Sample Position	Time(min) 0	16	30
A	0.1277	0.2866	0.3987
B	0.0747	0.2750	0.3751
C	0.0983	0.2455	0.3516
D	0.1100	0.2750	0.3692
μ	0.1027	0.2705	0.3735
s	0.0222	0.0176	0.0192

Table C-24. Pool concentration for Run No. 0.225-10887-696-B

Concentration in g moles/liter

Sample Position	Time(min) 0	6	14
A	0.2863	0.3809	0.5332
B	0.2925	0.3810	0.5793
C	0.2986	0.3693	0.5435
D	0.2927	0.3752	0.5377
μ	0.2926	0.3766	0.5484
s	0.0049	0.0056	0.0210

Table C-25. Pool concentration for Run No. 0.225-12667-0-S

Concentration in g moles/liter

Sample Position	Time(min) 0	13	21
A	0.0954	0.3384	0.4377
B	0.1142	0.3102	0.4230
C	0.1015	0.3159	0.4230
D	0.1015	0.3159	0.4343
μ	0.1031	0.3201	0.4295
s	0.0079	0.0125	0.0076

Table C-26. Pool concentration for Run No. 0.225-12667-942-B

Concentration in g moles/liter

Sample Position	Time(min) 0	8.5	16
A	0.0983	0.3396	0.5635
B	0.0803	0.3399	0.5460
C	0.0808	0.3398	0.5459
D	0.0919	0.3339	0.5576
μ	0.0878	0.3383	0.5532
s	0.0088	0.0029	0.0088

Table C-27. Pool concentration for Run No. 0.540-12226-0-S

Concentration in g moles/liter

Sample Position	Time(min) 0	25.5	46
A	0.1192	0.4327	0.6456
B	0.1026	0.3855	0.6144
C	0.1046	0.4044	0.6266
D	0.0860	0.4043	0.6323
μ	0.1031	0.4067	0.6297
s	0.0136	0.0195	0.0130

Table C-28. Pool concentration for Run No. 0.540-12226-366-B

Sample Position	Time(min) 0	15	24
A	0.0683	0.4174	0.6287
B	0.0334	0.4112	0.6248
C	0.0476	0.4053	0.6047
D	0.0581	0.3816	0.6542
μ	0.0518	0.4039	0.6281
s	0.0149	0.0157	0.0203

Table C-29. Pool concentration for Run No. 0.540-16130-0-S

Concentration in g moles/liter

Sample Position	Time(min) 0	6.5	12
A	0.2670	0.4389	0.5585
B	0.2024	0.4444	0.5572
C	0.2486	0.4146	0.5675
D	0.2442	0.4212	0.6162
μ	0.2405	0.4298	0.5748
s	0.0273	0.0142	0.0279

Table C-30. Pool concentration for Run No. 0.540-16130-637-B

Concentration in g moles/liter

Sample Position	Time(min) 0	5	9
A	0.0689	0.2738	0.4299
B	0.0828	0.2408	0.4453
C	0.0751	0.2970	0.4352
D	0.0772	0.2650	0.4270
μ	0.0760	0.2691	0.4344
s	0.0057	0.0232	0.0081

Table C-31. Pool concentration for Run No. 0.540-19643-0-S

Concentration in g moles/liter

Sample Position	Time(min) 0	5	9.5
A	0.4046	0.6933	0.9266
B	0.3987	0.6874	0.9322
C	0.4279	0.7050	0.9322
D	0.3751	0.6874	0.9205
μ	0.4016	0.6933	0.9279
s	0.0217	0.0083	0.0053

Table C-32. Pool concentration for Run No. 0.540-19643-944-B

Concentration in g moles/liter

Sample Position	Time(min) 0	3	7.5
A	0.2277	0.5634	0.9906
B	0.2284	0.6436	0.9620
C	0.3217	0.4918	1.043
D	0.2691	0.5689	1.0270
μ	0.2617	0.5669	1.0057
s	0.0444	0.0620	0.0364

Table C-33. Pool concentration for Run No. 0.680-10949-0-S

Concentration in g moles/liter

Sample Position	Time(min) 0	13.5	23
A	0.0390	0.1523	0.2378
B	0.0226	0.1643	0.2198
C	0.0136	0.1692	0.2261
D	0.0339	0.1692	0.2200
μ	0.0273	0.1637	0.2259
s	0.0114	0.0080	0.0084

Table C-34. Pool concentration for Run No. 0.680-10949-233-B

Concentration in g moles/liter

Sample Position	Time(min) 0	10	20
A	0.1920	0.4061	0.4377
B	0.1918	0.4061	0.4681
C	0.1805	0.4061	0.4230
D	0.2095	0.4029	0.4343
μ	0.1934	0.4053	0.4408
s	0.0118	0.0016	0.0193

Table C-35. Pool concentration for Run No. 0.680-14359-0-S

Concentration in g moles/liter

Sample Position	Time(min) 0	11	20
A	0.1692	0.3689	0.4907
B	0.1241	0.3400	0.5020
C	0.1467	0.3650	0.5189
D	0.1467	0.3441	0.5020
μ	0.1465	0.3545	0.5034
s	0.0184	0.0146	0.0116

Table C-36. Pool concentration for Run No. 0.680-14359-401-B

Concentration in g moles/liter

Sample Position	Time(min) 0	11	20
A	0.1406	0.2820	0.3779
B	0.1410	0.2933	0.3892
C	0.1354	0.2933	0.3835
D	0.1410	0.3049	0.3723
μ	0.1395	0.2934	0.3807
s	0.0027	0.0093	0.0073

Table C-37. Equilibrium Concentration Determination, C* at 21.1°C and 770 mm Hg.

Sample No. 1 C* = 17.24 g moles/liter

Sample No. 2 C* = 17.71 g moles/liter

Sample No. 3 C* = 17.57 g moles/liter

Sample No. 4 C* = 17.73 g moles/liter

Average C* = 17.56 g moles/liter

Standard Deviation = 0.15 g moles/liter

C* = 17.56 ± 0.15 g moles/liter

Table C-38. Surface Absorption

Run Condition	TFS(ml/min)	95% Confidence Limits	Correlation Coefficient
0.225-10887-0-S	20.93	±12.82%	0.9838
0.225-12667-0-S	36.20	± 5.55%	0.9969
0.540-12226-0-S	26.68	± 4.67%	0.9978
0.540-16130-0-S	65.06	±10.85%	0.9883
0.540-19643-0-S	131.30	± 4.33%	0.9981
0.680-10949-0-S	20.05	±10.50%	0.9891
0.680-14359-0-S	41.51	± 6.75	0.9954

Table C-39. Bubble and Surface Absorption

Run Condition	Sum(ml/min)	95% Confidence Limits	Correlation Coefficient
0.225-10887-696-B	43.06	±11.06%	0.9879
0.225-12667-942-B	67.52	± 2.38%	0.9994
0.540-12226-366-B	55.63	± 4.66%	0.9978
0.540-16130-637-B	91.94	± 6.27%	0.9961
0.540-19643-944-B	234.33	± 9.72%	0.9906
0.680-10949-233-B	28.70	±30.01%	0.9200
0.680-14359-401-B	56.05	± 5.20%	0.9973

Table C-40. Absorption from Bubbles

Run Condition	TF(ml/min)	95% Confidence Limits
0.225-10887-696-B	22.13	±16.17%
0.225-12667-942-B	31.32	± 4.31%
0.540-12226-366-B	28.95	± 5.90%
0.540-16130-637-B	26.88	±11.40%
0.540-19643-944-B	103.03	±10.05%
0.680-10949-233-B	8.65	±30.61%
0.680-14359-401-B	14.54	±10.75%

APPENDIX D

Sample Calculations

The equilibrium concentration of ammonia C* from the literature will be calculated and compared to the experimentally determined C*.

Table D-1**

P_{NH_3} (mm Hg)	Ratio $\frac{g_{NH_3}}{g_{H_2O}}$
t = 20°C	
700	0.497
800	0.544
t = 40°C	
750	0.315
800	0.329

** Source of Data: Washburn, E.W., "International Critical Tables," (1928) 3:259.

All the runs were carried out at a total system pressure of 770 mm Hg and 21.1°C. The vapor pressure of water at 21.1°C = 18.76 mm Hg. Hence, P_{NH_3} = (770-18.76) mm Hg = 751.24 mm Hg.

From Table D-1, interpolating to 751.24 mm Hg and then extrapolating to 21.1°C, the ratio of $\frac{g_{NH_3}}{g_{H_2O}}$ is found to be 0.5101.

At P_{NH_3} = 751.24 mm Hg and t = 21.1°C,

$$\frac{g_{NH_3}}{g_{H_2O}} = 0.5101$$

Therefore,

$$\text{wt\% of } NH_3 \text{ in solution} = \frac{\text{wt. of } NH_3}{\text{total wt. of solution}} \times 100\%$$

$$= \frac{0.5101 \text{ g} \times 100\%}{1\text{g} + 0.5101 \text{ g}}$$

$$= 33.779\%$$

** Density of 33.78%

ammonia solution at 21.1°C = 0.8825 g/ml

** Source of Data: Perry, J. H. "Chemical Engineers Handbook," 1963. 4th edition.

$$\text{Volume of ammonia solution} = \frac{\text{total weight of solution}}{\text{density of solution}}$$

$$= \frac{1.5101 \text{ g}}{0.8825 \text{ g/ml}} = 1.7112 \text{ ml}$$

$$\text{g moles of } NH_3 \text{ in solution} = \frac{0.5101 \text{ g}_{NH_3}}{\frac{17 \text{ g}_{NH_3}}{\text{g mole } NH_3}} = 0.0300 \text{ g mole}$$

$$\text{Concentration of ammonia solution} = \frac{0.0300 \text{ g mole } NH_3}{1.7112 \text{ ml} \times 10^{-3} \frac{\text{lit}}{\text{ml}}}$$

$$= 17.5349 \frac{\text{g moles } NH_3}{\text{liter}}$$

Calculation of practical Henry's Law constant for ammonia

UNITS

$$N_A = k_G A(P-P^*)$$

$$\frac{\text{g mole}}{\text{min}} \qquad \text{(atm)}$$

$k_G A$ has units of $\frac{\text{g mole}}{(\text{min})(\text{atm})}$

$$P = HC^*$$

$$\text{atm} \qquad \frac{\text{g mole}}{\text{ml}}$$

H, the Henry's Law constant, has units of $\frac{(\text{atm})(\text{ml})}{\text{g moles}}$

$$H \times k_G A = \frac{(\text{atm})(\text{ml})}{(\text{g moles})} \times \frac{\text{g moles}}{(\text{min})(\text{atm})} = \frac{\text{ml}}{\text{min}}$$

Partial pressure of NH_3 for all the experimental runs = 751.24 mm Hg

$$P_{NH_3} = 0.98847 \text{ atm}$$

$$C^*(\text{experimental}) = 17.56 \frac{\text{g moles}}{\text{lit}}$$

$$= 0.01756 \frac{\text{g moles}}{\text{ml}}$$

FOR AMMONIA

$$H = \frac{0.98847 \text{ atm}}{0.01756 \frac{\text{g mole}}{\text{lit}}} = 56.29 \frac{(\text{atm})(\text{ml})}{\text{g mole}}$$

FOR OXYGEN#

C* for oxygen at 21.1°C and partial pressure of 0.98847 atm = 43.31×10^{-3} mg/ml

#Source of Data: Hauxwell (5)

$$C^*_{O_2} = 1.3534 \times 10^{-6} \frac{\text{g mole}}{\text{ml}} \quad \text{after conversion.}$$

$$H = \frac{0.98847 \text{ atm}}{1.3534 \times 10^{-6} \frac{\text{g moles}}{\text{lit}}} = 730{,}360 \frac{(\text{atm})(\text{ml})}{\text{g mole}}$$

Calculation of the pool concentration from the run data

The run data from 0.540-16130-637-B will be used to illustrate the procedure.

Concentration of H_2SO_4 = 3.1226 eq/lit

Concentration of NaOH = 3.0990 eq/lit

At time = 5 minutes and for the sample position B, we have:

Volume of H_2SO_4 used = 3.77 ml

Volume of NaOH used = 3.39 ml

Also for the experimental runs, the volume of ammonia analyzed to determine pool concentration was 5.26 ml.

eq NH_3 = eq H_2SO_4 - eq NaOH

$$\text{eq } NH_3 = (0.00377 \text{ lit})\left(3.1226 \frac{\text{eq}}{\text{lit}}\right) - (0.00339 \text{ lit})\left(3.0990 \frac{\text{eq}}{\text{lit}}\right)$$

eq NH_3 = 0.0012666

Now the following reaction takes place between the NH_3 and H_2SO_4.

$$NH_3 + H_2SO_4 = NH_4^+ + HSO_4^-$$

Thus, this reaction has a conversion ratio of

$$\frac{1 \text{ g mole } NH_3}{1 \text{ g eq } NH_3}$$

$$0.0012666 \text{ g eq } NH_3 \times \frac{1 \text{ g mole } NH_3}{1 \text{ g eq } NH_3} = 0.0012666 \text{ g mole}$$

Volume of solution = 0.00526 lit

$$\text{Concentration} = \frac{0.001266 \text{ g mole } NH_3}{0.00526 \text{ liter}}$$

$$= 0.2408 \frac{\text{g moles}}{\text{liter}}$$

Procedure for calculating TF

The calculation of TF requires the prior determination of the quantities, SUM and TFS. Recall that:

$$SUM = TF + TFS$$

Knowing the values of SUM and TFS, allows one to solve for the TF in the above equation. Data for Run No. 0.540-12226-0-S and Run No. 0.540-12226-366-B will be used to show the procedure for calculating TF. Note that for each run time in minutes and the pool concentration are given at four sample locations. We therefore have:

$$\text{pool concentration} = C(\text{sample position, time})$$

The pool concentration as given above has units of g moles per liter of solution. The dimensionless concentraion, C^+(sample position, time) is obtained by dividing C(sample position, time) with the equilibrium concentration, C*. C* is equal to 17.56 g moles per liters of solution.

In other words, one obtains:

$$C^+(\text{sample position, time}) = \frac{C(\text{sample position, time})}{C^*}$$

From now on, sample position will simple be referred to as position.

$$C^+(\text{position, time}) = \frac{C(\text{position, time})}{17.56}$$

From Run No. 0.540-12226-0-S, for time equal to 25.5 minutes and sample position D. The pool concentration is listed as $0.4043 \frac{\text{g mole}}{\text{liter}}$.

$$C(D, 25.5) = 0.4043 \frac{\text{g moles}}{\text{liter}}$$

$$C^{+}(D, 25.5) = \frac{C(D, 25.5)}{C^{*}}$$

$$C^{+}(D, 25.5) = \frac{0.4043}{17.56} = 0.0230$$

The mean of the four readings of the pool concentration at time equal to zero minutes is used in calculating C_o.

$$C_o = C(\text{mean}, 0)$$

$$C_o^{+} = \frac{C(\text{mean}, 0)}{17.56}$$

For Run No. 0.540-12226-0-S

$$C_o^{+} = \frac{0.1031}{17.56} = 0.0059$$

Using the above procedure, tabulated values for Run No. 0.540-12226-0-S and Run No. 0.540-12226-366-B are listed below.

Table D-2. C^{+}(position, time) for Run No. 0540-1226-0-S

Sample Position	Time(min) 0	25.5	46
A	0.0068	0.0246	0.0368
B	0.0058	0.0220	0.0350
C	0.0060	0.0230	0.0357
D	0.0049	0.0230	0.0360

$$C_o^{+} = 0.0059$$

Table D-3. C^+(position, time) for Run No. 0.540-12226-366-B

Sample Position	Time(min) 0	15	24
A	0.0039	0.0238	0.0358
B	0.0019	0.0234	0.0356
C	0.0027	0.0231	0.0344
D	0.0033	0.0217	0.0372

$$C_o^+ = 0.0029$$

Now compute the quantity, $\ell n \dfrac{1 - C_o^+}{1 - C^+}$

using Run No. 0.540-12226-0-S and Run No. 0.540-12226-366-B.

Let $Y = \ell n \dfrac{1 - C_o^+}{1 - C^+}$.

Table D-5. Y for Run No. 0.540-12226-366-B

Sample Position	Time(min) 0	15	24
A	0.001003	0.021183	0.033552
B	-0.001002	0.020774	0.033345
C	-0.000201	0.020467	0.032101
D	0.000401	0.019034	0.035005

Table D-4. Y for Run No. 0.540-12226-0-S

Sample Position	Time(min 0	25.5	46
A	0.000906	0.018990	0.031577
B	-0.000101	0.016328	0.029709
C	0.000100	0.017351	0.030435
D	-0.001005	0.017351	0.030746

Recall that for Run No. 0.540-12226-0-S, in which no bubbles were entrained, the model developed predicts a relationship of the following form.

$$Y = \ln \left[\frac{1 - C_o^+}{1 - C^+} \right] = \frac{TFS}{V} t$$

The above equation predicts that a plot of Y versus t should give a straight line on a rectilinear graph paper. The slope of the straight line will be equal to $\frac{TFS}{V}$, with an intercept equal to zero. The data was fitted using the least square fit method. The constants a and b were chosen so that,

$$\sum_{i=1}^{12} \left[y_i - (a + bx_i) \right]^2$$

is a minimum.

$y_i = Y_i$ (specific value of Y)

$x_i = t_i$ (time corresponding to y_i)

Thus, we obtain:

$$S_{xx} = 12 \sum_{i=1}^{12} x_i^2 - \left[\sum_{i=1}^{12} x_i \right]^2$$

$$S_{yy} = 12 \sum_{i=1}^{12} y_i^2 \cdot - \left[\sum_{i=1}^{12} y_i\right]^2$$

$$S_{xy} = 12 \sum_{i=1}^{12} x_i y_i - \left[\sum_{i=1}^{12} x_i\right]\left[\sum_{i=1}^{12} y_i\right]$$

The constants are given as:

$$a = \bar{y} - b(\bar{x})$$

$$b = \frac{S_{xy}}{S_{xx}}$$

where:

$$\bar{y} = \frac{\left[\sum_{i=1}^{12} y_i\right]}{12}$$

$$\bar{x} = \frac{\left[\sum_{i=1}^{12} x_i\right]}{12}$$

The following values are obtained.

$$a = 0.00017$$

$$b = 0.00067$$

Thus, the final equation of interest is

$$Y = 0.00017 + 0.00067\ t$$

where

$$Y = \ell n\left[\frac{1 - C_o^+}{1 - C^+}\right]$$

t = time in minutes

The variance, S_e^2, is given as:

$$S_e^2 = \frac{S_{xx}\, S_{yy} - (S_{xy})^2}{12(12-2)(S_{xx})} = 0.00000082$$

The 95% confidence limit for the slope is given by:

$$b \pm \frac{t_{0.025}^{d.f.s} \cdot S_e \cdot \sqrt{\frac{12}{S_{xx}}}}{b} \times 100\%$$

d.f.s = degrees of freedom = 12-2 = 10

$t_{0.025}^{10}$ = value of student "t" distribution

The 95% confidence limit on slope:

$0.00067 \pm 4.67\%$

Therefore, the 95% confidence limit on TFS is:

$$TFS = 26.68 \pm 4.67\% \ \frac{ml}{min}$$

The correlation coefficient, r:

$$r = \frac{S_{xy}}{\sqrt{S_{xx} \cdot S_{yy}}} = 0.9978$$

Similarly for Run No. 0.540-12226-366-B in which bubbles are entrained, the following results are obtained using the above procedure.

$Y = -0.00015 + 0.00139\ t$

$$SUM = 55.63 \pm 4.66\% \ \frac{ml}{min}$$

Correlation coefficient, r = 0.9978

The 95% confidence limits on TF were determined by summing the variances of both TF and SUM.

$$\text{Confidence limits} = \pm\left(\frac{t^{d.f.c}_{0.025}\sqrt{V_{art}}\sqrt{\frac{n}{S_{xx}}}}{\text{SLOPE}}\right) \times 100\%$$

where:

$V_{art} = V_{ars} + V_{ar}$

V_{ars} = variance from Run No. 0.540-12226-0-S

V_{ar} = variance from Run No. 0.540-12226-366-B

d.f.c = approximate degrees of freedom to be calculated

SLOPE = slope of $\ell n\left[\frac{1 - C_o^+}{1 - C^+}\right] V_s$ t obtained from Run No. 0.540-12226-366-B

n = 12

d.f.c = approximate degree of freedom = $\left[\frac{(V_{art})^2}{\frac{(V_{ars})^2}{d.f.s} + \frac{(V_{ar})^2}{d.f.b}}\right]$

d.f.s = degree of freedom for Run No. 0.540-12226-0-S

d.f.b = degree of freedom for Run No. 0.540-12226-366-B

From Run No. 0.540-12226-0-S

$V_{ars} = 0.82 \times 10^{-6}$

d.f.s = 10

From Run No. 0.540-12226-366-B

$$V_{ar} = 0.99 \times 10^{-6}$$

$$d.f.b = 10$$

$$V_{art} = V_{ars} + V_{ar} = 1.81 \times 10^{-6}$$

$$d.f.c = \left[\frac{(1.81 \times 10^{-6})^2}{\frac{(0.82 \times 10^{-6})^2}{10} + \frac{(0.99 \times 10^{-6})^2}{10}} \right] = 19.82$$

Use 19 degress of freedom

$$d.f.c = 19$$

$t^{19}_{0.025}$ = Value of student 't' distribution

$$= 2.093$$

$$S_{xx} = 14112$$

$$SLOPE = 0.00139$$

$$\text{Confidence limits} = \pm \frac{2.093(.001345)(.02916) \times 100\%}{0.00139}$$

on TF, %

$$= 5.90\%$$

$$TF = 28.95 \pm 5.90\% \ \frac{ml}{min}$$